

Single-Stranded DNA Functionalized Single-Walled Carbon Nanotubes for Microbiosensors via Layer-by-Layer Electrostatic Self-Assembly

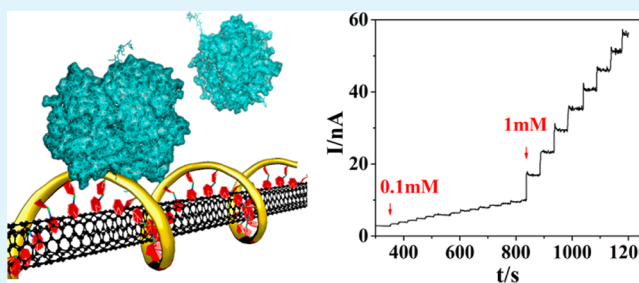
Zhuo Kang,^{†,‡} Xiaoqin Yan,[†] Yue Zhang,^{*,†,§} Jing Pan,^{||} Jin Shi,[‡] Xiaohui Zhang,[†] Yi Liu,[†] Jong Hyun Choi,^{||} and D. Marshall Porterfield^{*,‡}

[†]State Key Laboratory for Advanced Metals and Materials, School of Materials Science and Engineering, and [§]Key Laboratory of New Energy Materials and Technologies, University of Science and Technology Beijing, Beijing 100083, China

[‡]Physiological Sensing Facility and ^{||}School of Mechanical Engineering, Purdue University, West Lafayette, Indiana 47907, United States

ABSTRACT: In this letter, the facial noncovalent adsorption of single-stranded DNA (ssDNA) provided single-walled carbon nanotubes (SWNTs) with biofunctionality while their superior properties were retained. In this case, we innovatively demonstrated the feasibility of employing the negative surface charge of ssDNA-SWNTs to realize layer-by-layer electrostatic self-assembly. On the basis of such a sandwichlike structure, an applicable glucose microbiosensor with direct electrochemistry and high performance was fabricated. The proposed protocol provided an ideal platform for various sensing applications, and might have profound influence on related nanotechnology.

KEYWORDS: single-stranded DNA, single-walled carbon nanotube, electrostatic self-assembly, direct electrochemistry, biosensor



INTRODUCTION

Single-walled carbon nanotubes (SWNT) have recently been applied in a variety of nanoscale biosensor applications as the sensing element because of their unique physicochemical properties.^{1–4} However, their insolubility and tendency to aggregate greatly affect the formation of a thin and uniform SWNT film on the transducers' surface, which is regarded as one of the most crucial steps during the biosensor fabrication. To overcome this barrier, single-stranded DNA (ssDNA) was reported to significantly improve the solubility of SWNT in water,⁵ thus opening up a new approach for solution phase SWNT applications. Because ssDNA-SWNTs are individually suspended in water, the strains among any of the nanotubes to form the film are equivalent in all directions.⁶ As a result, the acquired nanotube film is uniform and adheres tightly to the electrode surface so that it will not easily fall off when dipped in solution. In addition, SWNTs have a relatively inert surface, which makes it difficult to modify their sidewall. Receptor molecules could only be immobilized on the edges of nanotubes through covalent bonds.⁷ Although with acid or alkali treatment, SWNT could be modified with some active functional groups on the sidewall, there is no doubt this process would potentially damage the surface crystal structure of SWNTs simultaneously, thus affecting their electrical property. Therefore, in order to immobilize receptor molecules to a great level, ssDNA is a good candidate to modify the side wall of SWNT without destructing its original structure and properties. It has been demonstrated that the redox overpotential was

reduced⁸ and the electroanalytical current was dramatically enhanced⁹ by incorporating ssDNA-SWNTs in electrochemical process. So far, ssDNA-SWNTs have been introduced in biosensors for the detection of glucose,¹⁰ proteins,¹¹ uric acid,¹² dopamine,^{12–14} and ascorbic acid.¹² Despite all the successful applications of ssDNA-SWNTs in biosensors, few researchers have exploited the negative surface charge of ssDNA-SWNTs complex for biosensor construction via electrostatic interactions and biosensing enhancement.

On the other hand, layer-by-layer (LBL) self-assembly is a simple and inexpensive technique of assembling ultrathin films of a variety of organic and inorganic compounds, which allows for the control of layer thickness in nanometer range.^{15–17} Recently, LBL self-assembly has been successfully employed for the design and construction of biosensors.^{18–24} It has been reported that LBL protocol not only facilitated the direct electron transfer between the redox sites and electrode, but also provided a satisfactory microenvironment for the enzymes.^{19,21,24–27}

Here we present a fundamentally new nanostructured biosensor based on ssDNA-SWNTs. By integrating the excellent properties of ssDNA-SWNTs with the advantages of LBL electrostatic self-assembly, a novel glucose microbiosensor with direct electrochemistry was realized. Negatively charged

Received: January 7, 2014

Accepted: March 7, 2014

Published: March 7, 2014

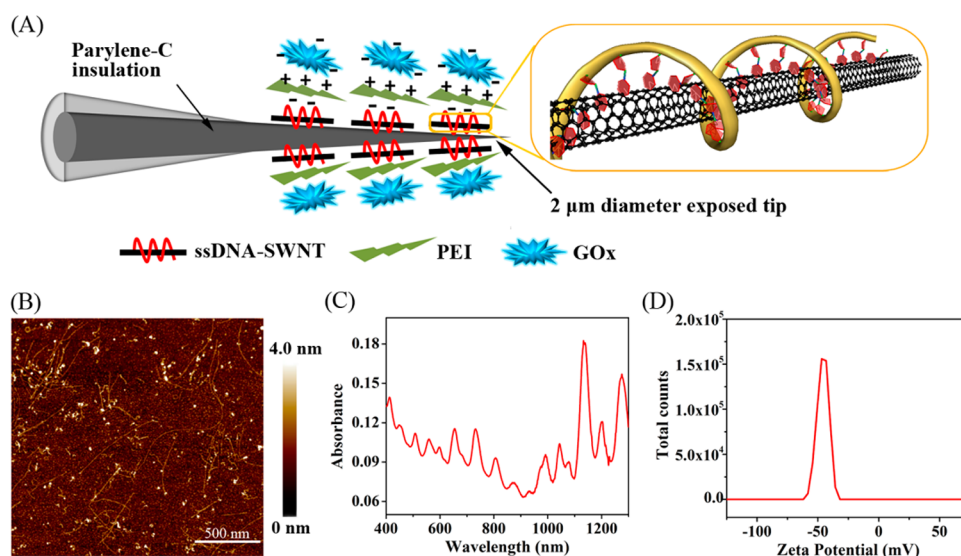


Figure 1. (A) Illustration diagram of LBL electrostatic self-assembly of ssDNA-SWNT, PEI, and GOx on Pt/Ir wire microelectrode. Inset: schematic of ssDNA-SWNT; (B) AFM image of individual ssDNA-SWNTs; (C) Vis–NIR adsorption spectra of dispersed ssDNA-SWNTs solution; (D) zeta potential graph of dispersed ssDNA-SWNTs solution. Inset is the comparison of dispersed ssDNA-SWNTs solution with deionized water.

Glucose oxidase (GOx) was effectively immobilized on the negatively charged ssDNA-SWNTs through a thin layer of cationic poly(ethylenimine) (PEI) (Figure 1A). Major parameters of the fabricated biosensors were characterized to demonstrate their further applications on the self-referencing system²⁸ in physiological sensing environment. More importantly, we initiated to explore the possibility of employing negatively charged ssDNA-SWNTs to do electrostatic self-assembly, which might have profound influence on related nanotechnology.

MATERIAL AND METHODS

Chemicals and Reagents. All solutions, if not specified, were prepared in deionized water (DI) of resistivity 18.2 MΩ·cm (Milli Q). Glucose oxidase (E.C.1.1.3.4, 100 000–250 000 units/g, from *Aspergillus niger*), sodium chloride (NaCl), potassium chloride (KCl), ascorbic acid, uric acid and acetaminophen were purchased from Sigma Aldrich.

Dispersion of SWNTs Using ssDNA. HiPco SWNTs (Unidym, Sunnyvale, CA) were mixed with an aqueous solution of single-stranded, 30 base-long poly T oligonucleotides (Integrated DNA Technologies, Coralville, IA). The initial concentration of SWNTs was 200 mg/L. Then the mixture was sonicated for 1 h and centrifugated for 30 000 rpm for 150 min to remove impurities, aggregates and bundles, leaving the acquired solution at a concentration estimated to be around 30 mg/L (≈15% of the original suspension) which is determined by measuring its absorption at 633 nm ($\epsilon_{\text{SWNT}} = \sim 0.036 \times 10^5 \text{ L mg}^{-1} \text{ cm}^{-1}$).²⁹

AFM Characterization. Fifty microliters of diluted sample solution was deposited on a SiO₂ substrate. After 30 min, it was thoroughly rinsed with DI and dried with N₂ steam. Tapping mode was used to acquire an image under ambient conditions (Bruker Dimension Icon AFM system)

Fabrication of Microbiosensors. A Pt/Ir wire microelectrode (PI20033.0A10, 51 mm length, 0.256 mm shaft diameter, 1–2 μm tip diameter, 3 μm parylene-C coated metal shaft) (Figure 1A), on which the ssDNA-SWNT, PEI, and GOx were successively deposited through layer-by-layer

electrostatic self-assembly, was used to fabricate the microbiosensor. First of all, the ssDNA-SWNT solution (2 μL) was cast on the tip of the microelectrode using a pipet, and the microelectrode was subsequently air-dried for 10 min to form a thin and uniform SWNT layer on the tip. GOx was immobilized on the negatively charged ssDNA-SWNT surface through a layer of positively charged PEI. Prior to it, the detailed experimental parameters were optimized. It was found that the optimal and reasonable immersing time for the assembly of PEI and GOx layers was 2 and 10 min, respectively. On this basis, the microelectrode covered with ssDNA-SWNT was dipped in PEI solution (MW 60 000, 3 wt %) for 2 min. After it was rinsed with DI and dried in nitrogen steam, a cationic layer of PEI was acquired. Then the resulted PEI/ssDNA-SWNTs electrode was dipped into GOx solution (10 mg/mL) for 10 min at 4 °C. During this period, the negatively charged GOx (PI = 4.6) molecules were adsorbed to the positively charged PEI surface through electrostatic interaction. The loosely attached GOx molecules were removed by a thorough rinse with DI, followed by air-dried for 10 min. The obtained GOx/PEI/ssDNA-SWNTs microelectrodes were then kept at 4 °C in refrigerator when not in use.

RESULTS AND DISCUSSION

DNA has been demonstrated to be very effective at dispersing SWNTs in aqueous solutions because of its amphiphilic nature. For ssDNA-SWNTs (Figure 1A, inset), a model proposed that the helical form DNA can wrap around a nanotube, and the hydrophobic nitrogen bases are adsorbed to the nanotube surface via noncovalent π – π stacking while the hydrophilic sugar phosphate backbone is directed into water.^{5,30} To characterize the dispersion quality, we employed atomic force microscopy (AFM). The AFM image (Figure 1B) shows that ssDNA-SWNTs have a length distribution from 50 to 1000 nm, with nanotube diameter ranging from 1.2 to 2.3 nm which is larger than the expect value of 0.7 to 1.1 nm for HiPco nanotubes.^{31,32} However, the results are consistent with DNA coated nanotubes.⁵ The individual nanotubes on substrate demonstrate good dispersion rather than aggregation. In the

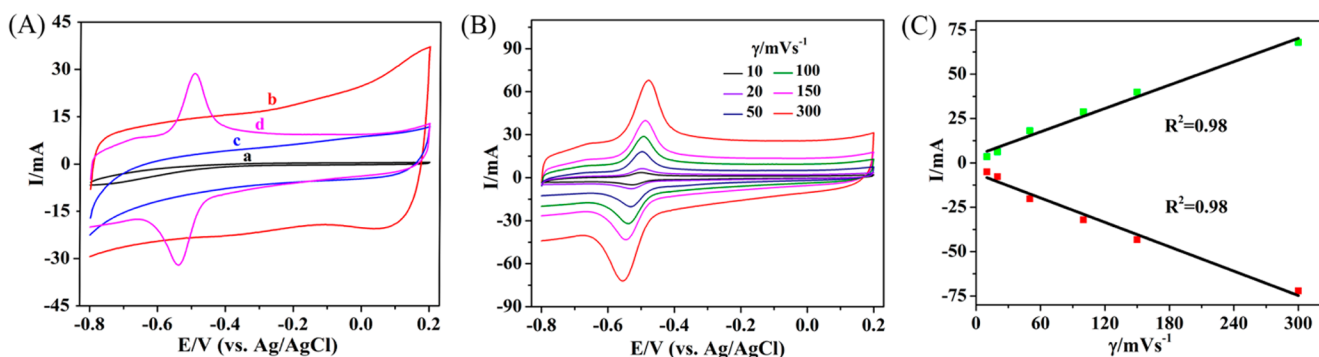


Figure 2. (A) Cyclic voltammograms of different modification of standard Pt electrodes in pH 7.0 deoxygenated PBS at a scan rate of 100 mV/s. (a) Bare Pt electrode, (b) ssDNA-SWNTs/Pt, (c) PEI/ssDNA-SWNTs/Pt, (d) GOx/PEI/ssDNA-SWNTs/Pt; (B) cyclic voltammograms of GOx/PEI/ssDNA-SWNTs/Pt in pH 7.0 deoxygenated PBS at 10, 20, 50, 100, 150, and 300 mV/s. (C) Dependence of anodic and cathodic peak current on scan rates.

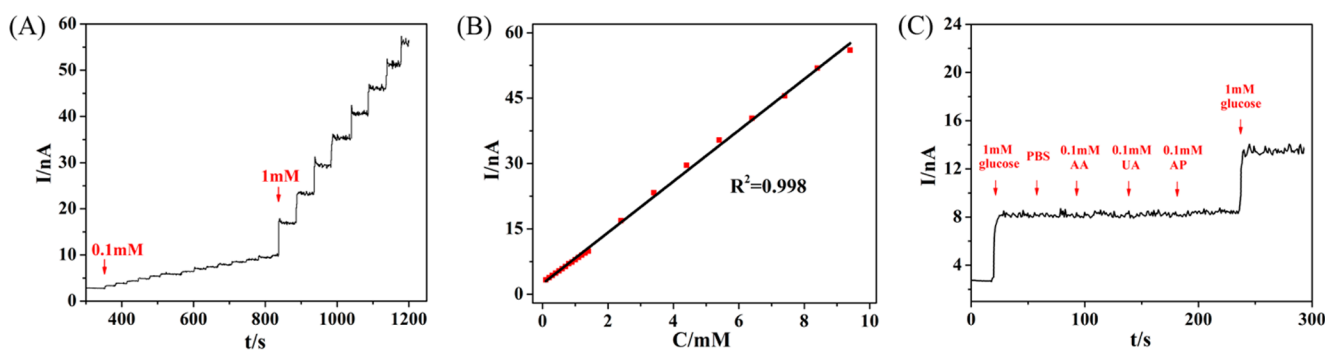


Figure 3. (A) Amperometric responses of the GOx/PEI/ssDNA-SWNTs/Pt microprobe at +500 mV (vs Ag/AgCl) upon successive addition of glucose solution to 20 mL of pH 7.0 PBS stirred at 350 rpm. (B) Calibration curve of amperometric response toward glucose concentration variation. (C) Amperometric responses to PBS, 0.1 mM AA, 0.1 mM UA, 0.1 mM AP, and 1 mM glucose for fabricated microprobe.

absorption spectra (Figure 1C), the well-defined peaks also suggest lack of large aggregation in the solution by removing bundles through centrifugation. Nevertheless, the absorption features of aggregated SWNTs sample are red-shifted and broadened (data not shown here).

More importantly, DNA is negatively charged due to the phosphate group. For zeta potential measurement of ssDNA-SWNT (Figure 1D), a single and sharp peak with a peak width of 4.7 mV indicates a uniform charge distribution on SWNT surface. The mean value of zeta potential is -45.9 mV at 25 °C, demonstrating ssDNA-SWNT is negatively charged, and thus theoretically proved the feasibility of electrostatic LBL self-assembly.

In order to characterize the GOx/PEI/ssDNA-SWNT multilayer assembly process, cyclic voltammetric measurement of different modification of standard Pt electrode ($d = 2$ mm) were performed in pH 7.0 deoxygenated PBS at the scan rate of 100 mV/s (Figure 2A). For bare Pt (curve a), ssDNA-SWNTs/Pt (curve b), and PEI/ssDNA-SWNTs/Pt (curve c) electrodes, they only contain nonfaradic current in the applied potential window. However, from a to b, the background current increases significantly due to the large specific area of nanotubes after ssDNA-SWNTs are deposited.^{24,33} From b to c, after PEI is adsorbed onto the ssDNA-SWNTs/Pt electrode, the back current decreases, which may be ascribed to the nonconductivity of PEI. For curve d, with another layer of GOx adsorbed on PEI through electrostatic interaction, a pair of well-defined redox peaks is observed, indicating good electron transfer of stably fixed GOx. However, when the layer number

for each component was increased to two, the current response decreased by an order of magnitude due to the nonconductive PEI. Therefore, only one layer for each component was adopted for this configuration.

Figure 2B shows cyclic voltammograms of GOx/PEI/ssDNA-SWNTs/Pt in pH 7.0 deoxygenated PBS from 10 to 300 mV/s. The anodic and cathodic peak currents increase linearly with an increase of the scan rate, which is characteristic of a surface-controlled electrochemical process. Besides, taking 50 mV/s for example, anodic peak potential ($E_{p,a}$) and cathodic peak potential ($E_{p,c}$) are respectively -0.497 and -0.532 V with a small peak potential separation (ΔE_p) of 35 mV, revealing a fast electron transfer process. Additionally, the formal potential ($E_0 = 1/2 (E_{p,a} + E_{p,c})$) of the redox couple is calculated to be -0.514 V, which is close to the standard electrode potential for FAD/FADH₂ at pH 7.0. Meanwhile, the anodic peak current is almost equal to the cathodic peak current, suggesting a quasi-reversible process. All these results demonstrate a direct electrochemistry reaction is achieved, which can be attributed to the more detailed nanostructure formed by ssDNA-SWNTs because of the excellent dispersion of SWNTs in aqueous solution.

According to the Laviron equation,³⁴ the concentration of electroactive GOx (Γ , mol cm⁻²) outside the PEI layer was estimated to be 8.27×10^{-10} mol cm⁻², which is much higher than the theoretical value of 2.86×10^{-12} mol cm⁻² for the monolayer of GOx on the bare electrode surface. Furthermore, compared with other reports based on carbon nanotubes with direct electrochemistry, such as 8.77×10^{-11} mol cm⁻² for

CdTe quantum dots/carbon nanotubes electrodes,³⁵ 2.56×10^{-10} mol cm⁻² for biomediated gold nanoparticles/multi-walled carbon nanotubes (MWNTs) electrode³⁶ and 4.7×10^{-10} mol cm⁻² even for GOx/PEI/MWNTs electrode through LBL assembly,²⁴ the result we acquired has certain advantages.

The electron transfer rate constant (K_s) was estimated to be 1.58 s^{-1} which is extremely close to 1.61 s^{-1} for GOx directly adsorbed on carbon nanotubes powder microelectrode,³⁷ demonstrating the introduction of a thin PEI layer does not have significant effect on electron transfer. Moreover, this value is larger than 0.91 s^{-1} for DNA/Chitosan film based electrode³⁸ and 1.01 s^{-1} for carbon nanotube-gold colloid modified electrode.³⁹ The results indicate multilayers tightly combined through electrostatic interaction can provide more specific surface area for enzyme loading and a suitable microenvironment that facilitates the electron transfer between GOx and electrode.

The amperometric response performance of fabricated microelectrode was evaluated at applied potential of +500 mV in stirring PBS with successive addition of glucose (Figure 3A). The time required to reach 95% of the steady-state current was within 3s. Figure 3B is the calibration curve of steady-state current vs glucose concentration. The sensitivity was calculated to be 6 nA/mM that is much larger than 0.53 nA/mM for the same kind of Pt/Ir microelectrode modified with Platinum black, MWNTs and Nafion,⁴⁰ 0.43 nA/mM for a carbon fiber microelectrode modified with ruthenium and GOx,⁴¹ and 7 pA/mM for a microsensor with 8 μm tip diameter.⁴² The detection limit was estimated to be 38 μM at a signal-to-noise ratio (S/N) of 3. The linear range was up to 9.4 mM with a correlation coefficient of 0.998, which covered glucose concentration of around 5 mM in normal human blood and many cell culture medias such as 5.5 mM in mesenchymal stem cell basal medium,⁴³ indicating an obvious improvement over previously reported microbiosensors^{41,42,44} or carbon nanotube based glucose biosensors.^{45,46} This could be attributed to the huge surface area of the more detailed 3D structured formed by ssDNA-SWNTs, which is more favorable for immobilization of large amount of active GOx molecules, consisting with the calculated concentration of electroactive GOx (Γ).

The microprobe also exhibited a high selectivity over electroactive, interfering species commonly found in human serum samples. As shown in Figure 3C, between two obvious steps came from 1 mM glucose increasement, addition of PBS solution, Ascorbic acid (AA), uric acid (UA) and acetaminophen (AP) were injected. The response to 0.1 mM AA and 0.1 mM UA were 0.7% and 0.8% that of 1 mM glucose, whereas PBS solution and 0.1 mM AP did not cause obvious current change, demonstrating the microprobe has an acceptable anti-interference ability, and thus is promising for applications in physiological environment. After the fabricated microprobes were stored at 4 °C for 3 weeks, they retained 91% of their original current responses. Meanwhile the relative standard deviation (R.S.D) of the response to 0.1 mM glucose was 2.6% for ten successive measurements. The R.SD for detection of 0.1 mM glucose with 6 different probes under the same conditions was 5.1%. Unlike other reported work,^{40,45,47} even without permselective membrane such as Nafion working as a protective layer or stable support matrix such as PEDOT, the result we obtained still indicated good selectivity, stability, and reproducibility. This can be ascribed to the LBL fabrication process that stabilizes the biosensor structure through electrostatic interaction between each layer.

CONCLUSION

We have initiatively demonstrated the example of using ssDNA-SWNTs through LBL layer self-assembly technique in an electrochemical biosensing application. The well dispersed ssDNA-SWNTs formed a more detailed 3D nanostructure which is beneficial for realizing direct electrochemistry of GOx with extended linear range up to 9.4 mM and enhanced sensitivity of 6 nA/mM. Furthermore, we innovatively introduce ssDNA-SWNTs into electrostatic self-assembly by taking advantage of its negative charge. The sandwich structure acquired through adsorption of oppositely charged layers is favorable for steady immobilization of a large amount of GOx and enhancement of stability and anti-interference ability of the biosensor. Further research is underway to perfect ssDNA-SWNT-based electrostatic self-assembly nanostructure as a promising platform for versatile practical sensing applications.

AUTHOR INFORMATION

Corresponding Authors

*E-mail: yuezhang@ustb.edu.cn.

*E-mail: porterf@purdue.edu.

Notes

The authors declare no competing financial interest.

ACKNOWLEDGMENTS

This work was supported by the National Major Research Program of China (2013CB932602), the Major Project of International Cooperation and Exchanges (2012DFA50990), the Program of Introducing Talents of Discipline to Universities, the National Natural Science Foundation of China (51232001, 51172022, 51372023), the Research Fund of Co-construction Program from Beijing Municipal Commission of Education, the Fundamental Research Funds for the Central Universities, the Program for Changjiang Scholars and Innovative Research Team in University. Zhuo Kang thanks the China Scholarship Council (CSC) (No. 201206460052) for fellowship support.

REFERENCES

- (1) Cao, Q.; Rogers, J. A. Ultrathin Films of Single-Walled Carbon Nanotubes for Electronics and Sensors: A Review of Fundamental and Applied Aspects. *Adv. Mater.* **2009**, *21*, 29–53.
- (2) Barone, P. W.; Strano, M. S. Reversible Control of Carbon Nanotube Aggregation for a Glucose Affinity Sensor. *Angew. Chem., Int. Ed.* **2006**, *45*, 8138–8141.
- (3) Jeng, E. S.; Moll, A. E.; Roy, A. C.; Gastala, J. B.; Strano, M. S. Detection of DNA Hybridization Using the Near-Infrared Band-Gap Fluorescence of Single-Walled Carbon Nanotubes. *Nano Lett.* **2006**, *6*, 371–375.
- (4) Valentini, F.; Fernández, L. G.; Tamburri, E.; Pallechi, G. Single Walled Carbon Nanotubes/Polypyrrole-Gox Composite Films to Modify Gold Microelectrodes for Glucose Biosensors: Study of the Extended Linearity. *Biosens. Bioelectron.* **2013**, *43*, 75–78.
- (5) Zheng, M.; Jagota, A.; Semke, E. D.; Diner, B. A.; McLean, R. S.; Lustig, S. R.; Richardson, R. E.; Tassi, N. G. DNA-Assisted Dispersion and Separation of Carbon Nanotubes. *Nat. Mater.* **2003**, *2*, 338–42.
- (6) Hu, C.; Zhang, Y.; Bao, G.; Zhang, Y.; Liu, M.; Wang, Z. L. DNA Functionalized Single-Walled Carbon Nanotubes for Electrochemical Detection. *J. Phys. Chem. B* **2005**, *109*, 20072–20076.
- (7) Nguyen, T. T. T.; Simon, F. X.; Schmutz, M.; Mesini, P. J. Direct Functionalization of Self-Assembled Nanotubes Overcomes Unfavorable Self-Assembling Processes. *Chem. Commun.* **2009**, 3457–3459.
- (8) Xian, H.; Wang, P.; Zhou, Y.; Lu, Q.; Wu, S.; Li, Y.; Wang, L. Electrochemical Determination of Nitrite via Covalent Immobilization

of a Single-Walled Carbon Nanotubes and Single Stranded Deoxyribonucleic Acid Nanocomposite on a Glassy Carbon Electrode. *Microchim. Acta* **2010**, *171*, 63–69.

(9) Napier, M. E.; Hull, D. O.; Thorp, H. H. Electrocatalytic Oxidation of DNA-Wrapped Carbon Nanotubes. *J. Am. Chem. Soc.* **2005**, *127*, 11952–11953.

(10) Shi, J.; Cha, T. G.; Claussen, J. C.; Diggs, A. R.; Choi, J. H.; Porterfield, D. M. Microbiosensors Based on DNA Modified Single-Walled Carbon Nanotube and Pt Black Nanocomposites. *Analyst* **2011**, *136*, 4916–4924.

(11) Wu, Z.; Zhen, Z.; Jiang, J. H.; Shen, G. L.; Yu, R. Q. Terminal Protection of Small-Molecule-Linked DNA for Sensitive Electrochemical Detection of Protein Binding via Selective Carbon Nanotube Assembly. *J. Am. Chem. Soc.* **2009**, *131*, 12325–12332.

(12) Li, Y.; Wang, P.; Li, F.; Huang, X.; Wang, L.; Lin, X. Covalent Immobilization of Single-Walled Carbon Nanotubes and Single-Stranded Deoxyribonucleic Acid Nanocomposites on Glassy Carbon Electrode: Preparation, Characterization, and Applications. *Talanta* **2008**, *77*, 833–838.

(13) Ma, Y.; Ali, S. R.; Doodoo, A. S.; He, H. Enhanced Sensitivity for Biosensors: Multiple Functions of DNA-Wrapped Single-Walled Carbon Nanotubes in Self-Doped Polyaniline Nanocomposites. *J. Phys. Chem. B* **2006**, *110*, 16359–65.

(14) Li, J.; Wei, W.; Luo, S. A Novel One-Step Electrochemical Codeposition of Carbon Nanotubes-DNA Hybrids and Tiron Doped Polypyrrole for Selective and Sensitive Determination of Dopamine. *Microchim. Acta* **2010**, *171*, 109–116.

(15) Zhao, J.; Pan, F. S.; Li, P.; Zhao, C. H.; Jiang, Z. Y.; Zhang, P.; Cao, X. Z. Fabrication of Ultrathin Membrane via Layer-by-Layer Self-assembly Driven by Hydrophobic Interaction Towards High Separation Performance. *ACS Appl. Mater. Interfaces* **2013**, *5*, 13275–13283.

(16) Manna, U.; Patil, S. Glucose-Triggered Drug Delivery from Borate Mediated Layer-by-Layer Self-Assembly. *ACS Appl. Mater. Interfaces* **2010**, *2*, 1521–1527.

(17) Wang, X. L.; Jiang, Z. Y.; Shi, J. F.; Liang, Y. P.; Zhang, C. H.; Wu, H. Metal-Organic Coordination-Enabled Layer-by-Layer Self-Assembly to Prepare Hybrid Microcapsules for Efficient Enzyme Immobilization. *ACS Appl. Mater. Interfaces* **2012**, *4*, 3476–3483.

(18) Hodak, J.; Etchenique, R.; Calvo, E. J.; Singhal, K.; Bartlett, P. N. Layer-by-Layer Self-Assembly of Glucose Oxidase with a Poly-(allylamine)ferrocene Redox Mediator. *Langmuir* **1997**, *13*, 2708–2716.

(19) Wang, Y.; Joshi, P. P.; Hobbs, K. L.; Johnson, M. B.; Schmidtke, D. W. Nanostructured Biosensors Built by Layer-by-Layer Electrostatic Assembly of Enzyme-Coated Single-Walled Carbon Nanotubes and Redox Polymers. *Langmuir* **2006**, *22*, 9776–9783.

(20) Iost, R. M.; Crespilho, F. N. Layer-by-Layer Self-Assembly and Electrochemistry: Applications in Biosensing and Bioelectronics. *Biosens. Bioelectron.* **2012**, *31*, 1–10.

(21) Wu, B. Y.; Hou, S. H.; Yin, F.; Zhao, Z. X.; Wang, Y. Y.; Wang, X. S.; Chen, Q. Amperometric Glucose Biosensor Based on Multilayer Films via Layer-by-Layer Self-Assembly of Multi-Wall Carbon Nanotubes, Gold Nanoparticles and Glucose Oxidase on the Pt Electrode. *Biosens. Bioelectron.* **2007**, *22*, 2854–2860.

(22) Yang, M.; Yang, Y.; Yang, H.; Shen, G.; Yu, R. Layer-by-Layer Self-Assembled Multilayer Films of Carbon Nanotubes and Platinum Nanoparticles with Polyelectrolyte for the Fabrication of Biosensors. *Biomaterials* **2006**, *27*, 246–255.

(23) Zhao, H.; Ju, H. Multilayer Membranes for Glucose Biosensing via Layer-by-Layer Assembly of Multiwall Carbon Nanotubes and Glucose Oxidase. *Anal. Biochem.* **2006**, *350*, 138–144.

(24) Deng, C.; Chen, J.; Nie, Z.; Si, S. A Sensitive and Stable Biosensor Based on the Direct Electrochemistry of Glucose Oxidase Assembled Layer-by-Layer at the Multiwall Carbon Nanotube-Modified Electrode. *Biosens. Bioelectron.* **2010**, *26*, 213–219.

(25) Shen, L.; Hu, N. Electrostatic Adsorption of Heme Proteins Alternated with Polyamidoamine Dendrimers for Layer-by-layer

Assembly of Electroactive Films. *Biomacromolecules* **2005**, *6*, 1475–1483.

(26) Hu, Y.; Sun, H.; Hu, N. Assembly of Layer-by-Layer Films of Electroactive Hemoglobin and Surfactant Didodecyltrimethylammonium Bromide. *J. Colloid Interface Sci.* **2007**, *314*, 131–140.

(27) Shi, G.; Sun, Z.; Liu, M.; Zhang, L.; Liu, Y.; Qu, Y.; Jin, L. Electrochemistry and Electrocatalytic Properties of Hemoglobin in Layer-by-Layer Films of SiO₂ with Vapor-Surface Sol-Gel Deposition. *Anal. Chem.* **2007**, *79*, 3581–3588.

(28) Shi, J.; McLamore, E. S.; Marshall Porterfield, D. Nanomaterial Based Self-Referencing Microbiosensors for Cell and Tissue Physiology Research. *Biosens. Bioelectron.* **2013**, *40*, 127–134.

(29) Pan, J.; Zhang, H. Y.; Cha, T.-G.; Chen, H. R.; Choi, J. H. Multiplexed Optical Detection of Plasma Porphyrins Using DNA Aptamer-Functionalized Carbon Nanotubes. *Anal. Chem.* **2013**, *85*, 8391–8396.

(30) O'Connell, M. J.; Boul, P.; Ericson, L. M.; Huffman, C.; Wang, Y.; Haroz, E.; Kuper, C.; Tour, J.; Ausman, K. D.; Smalley, R. E. Reversible Water-Solubilization of Single-Walled Carbon Nanotubes by Polymer Wrapping. *Chem. Phys. Lett.* **2001**, *342*, 265–271.

(31) Bronikowski, M. J.; Willis, P. A.; Colbert, D. T.; Smith, K. A.; Smalley, R. E. Gas-phase production of carbon single-walled nanotubes from carbon monoxide via the HiPco process: A parametric study. *J. Vac. Sci. Technol. A* **2001**, *19*, 1800–1805.

(32) Zhou, W.; Ooi, Y. H.; Russo, R.; Papanek, P.; Luzzi, D. E.; Fischer, J. E.; Bronikowski, M. J.; Willis, P. A.; Smalley, R. E. Structural Characterization and Diameter-Dependent Oxidative Stability of Single Wall Carbon Nanotubes Synthesized by the Catalytic Decomposition of CO. *Chem. Phys. Lett.* **2001**, *350*, 6–14.

(33) Liu, G.; Lin, Y. Biosensor Based on Self-Assembling Acetylcholinesterase on Carbon Nanotubes for Flow Injection/Amperometric Detection of Organophosphate Pesticides and Nerve Agents. *Anal. Chem.* **2006**, *78*, 835–843.

(34) Laviron, E. General Expression of the Linear Potential Sweep Voltammogram in the Case of Diffusionless Electrochemical Systems. *J. Electroanal. Chem. Interfacial Electrochem.* **1979**, *101*, 19–28.

(35) Liu, Q.; Lu, X.; Li, J.; Yao, X.; Li, J. Direct Electrochemistry of Glucose Oxidase and Electrochemical Biosensing of Glucose on Quantum Dots/Carbon Nanotubes Electrodes. *Biosens. Bioelectron.* **2007**, *22*, 3203–3209.

(36) Zhang, H.; Meng, Z.; Wang, Q.; Zheng, J. A Novel Glucose Biosensor Based on Direct Electrochemistry of Glucose Oxidase Incorporated in Biomediated Gold Nanoparticles–Carbon Nanotubes Composite Film. *Sens. Actuators B* **2011**, *158*, 23–27.

(37) Zhao, Y. D.; Zhang, W. D.; Chen, H.; Luo, Q. M. Direct electron transfer of glucose oxidase molecules adsorbed onto carbon nanotube powder microelectrode. *Anal. Sci.* **2002**, *18*, 939–941.

(38) Gu, T. T.; Zhang, Y.; Deng, F.; Zhang, J.; Hasebe, Y. Direct Electrochemistry of Glucose Oxidase and Biosensing for Glucose Based on DNA/Chitosan Film. *J. Environ. Sci.* **2011**, *23*, S66–S69.

(39) Yao, Y. L.; Shiu, K. K. Direct Electrochemistry of Glucose Oxidase At Carbon Nanotube-Gold Colloid Modified Electrode With Poly(Diallyldimethylammonium Chloride) Coating. *Electroanalysis* **2008**, *20*, 1542–1548.

(40) McLamore, E. S.; Shi, J.; Jaroch, D.; Claussen, J. C.; Uchida, A.; Jiang, Y.; Zhang, W.; Donkin, S. S.; Banks, M. K.; Buhman, K. K.; Teegarden, D.; Rickus, J. L.; Porterfield, D. M. A Self Referencing Platinum Nanoparticle Decorated Enzyme-Based Microbiosensor for Real Time Measurement of Physiological Glucose Transport. *Biosens. Bioelectron.* **2011**, *26*, 2237–2245.

(41) Kohma, T.; Oyamatsu, D.; Kuwabata, S. Preparation of Selective Micro Glucose Sensor without Permeable Membrane by Electrochemical Deposition of Ruthenium and Glucose Oxidase. *Electrochem. Commun.* **2007**, *9*, 1012–1016.

(42) Jung, S.-K.; Trimarchi, J. R.; Sanger, R. H.; Smith, P. J. S. Development and Application of a Self-Referencing Glucose Microsensor for the Measurement of Glucose Consumption by Pancreatic β -Cells. *Anal. Chem.* **2001**, *73*, 3759–3767.

(43) Weil, B. R.; Abarbanell, A. M.; Herrmann, J. L.; Wang, Y.; Meldrum, D. R. High Glucose Concentration in Cell Culture Medium Does Not Acutely Affect Human Mesenchymal Stem Cell Growth Factor Production or Proliferation. *Am. J. Physiol.: Regul. Integr. Comp. Physiol.* **2009**, *296*, R1735–R1743.

(44) Kurita, R.; Hayashi, K.; Fan, X.; Yamamoto, K.; Kato, T.; Niwa, O. Microfluidic Device Integrated with Pre-reactor and Dual Enzyme-Modified Microelectrodes for Monitoring in Vivo Glucose and Lactate. *Sens. Actuators B* **2002**, *87*, 296–303.

(45) Wang, Y.; Liu, L.; Li, M.; Xu, S.; Gao, F. Multifunctional carbon nanotubes for direct electrochemistry of glucose oxidase and glucose bioassay. *Biosens. Bioelectron.* **2011**, *30*, 107–111.

(46) Mani, V.; Devadas, B.; Chen, S.-M. Direct Electrochemistry of Glucose Oxidase at Electrochemically Reduced Graphene Oxide-Multiwalled Carbon Nanotubes Hybrid Material Modified Electrode for Glucose Biosensor. *Biosens. Bioelectron.* **2013**, *41*, 309–315.

(47) Claussen, J. C.; Kumar, A.; Jaroch, D. B.; Khawaja, M. H.; Hibbard, A. B.; Porterfield, D. M.; Fisher, T. S. Nanostructuring Platinum Nanoparticles on Multilayered Graphene Petal Nanosheets for Electrochemical Biosensing. *Adv. Funct. Mater.* **2012**, *22*, 3399–3405.